ENHANCED ELECTRICAL CONDUCTIVITY IN LASER-INDUCED GRAPHENE-SILICON CARBIDE LAMINATED NANOSHEETS FOR FLEXIBLE STRAIN SENSORS AND PULSE WAVE VELOCITY ASSESSMENT

Yixin Liu[1,2], Yanru Chen[1], Zhibiao Wang[1,2], and Min Zhang[1]*
[1] Shenzhen International Graduate School, Tsinghua University, CHINA and
[2] Tsinghua-Berkeley Shenzhen Institute, Tsinghua University, CHINA

2024 IEEE 37th International Conference on Micro Electro Mechanical Systems (MEMS) | 979-8-3503-5792-9/24/$31.00 ©2024 IEEE | DOI: 10.1109/MEMS58180.2024.10439534

ABSTRACT

The synthesis and integration methods of electrical materials are vital in Polydimethylsiloxane (PDMS)-based electronics and sensors. Here, we present a compact approach for the in-situ synthesis of laser-induced graphene-silicon carbide laminated nanosheets (LIG-SiC LNS) with enhanced electrical conductivity on a MoS_2-PDMS hybrid precursor by laser direct scribing. We developed a flexible resistive strain sensor utilizing the simplified fabrication process of LIG-SiC LNS. The distinctive structure of the material enhances both the gauge factor (GF) and the intrinsic self-temperature compensation capability of the strain sensor. The sensor exhibits a maximum GF deviation of 1.88% within 20-35 ℃ without algorithmic compensation. In an application example, the sensor was utilized for assessing human pulse wave velocity (PWV), revealing a minimal deviation of 0.6% compared to a commercial instrument.

KEYWORDS

Flexible strain sensor, Pulse wave velocity, Laser-induced graphene-silicon carbide, Laminated nanosheets, Self-temperature compensation.

INTRODUCTION

Flexible strain sensors play a crucial role in wearable and implantable electronics, enabling the monitoring and diagnosis of human physiological signals. [1]. The sensors are generally fabricated by integrating flexible structural materials with electronic materials using various methods. Polydimethylsiloxane (PDMS) is widely used as the structural material for flexible electronics and sensors due to its favorable properties such as low Young's modulus (<10 MPa), stable chemical properties, transparency and fabricability [2]. Therefore, flexible resistive strain sensors based on PDMS for wearable electronics and health monitoring have attracted much attention [3]. PDMS is commonly employed as substrate or matrix material for the flexible sensors. Electronically functional materials, such as carbon nanotube [4], metal nanowire [5] and laser-induced graphene (LIG) [6], are often integrated with PDMS to enhance the functionalities and performance of the sensors.

LIG has been confirmed to be synthesized on various precursor materials by laser direct scribing [7], which has excellent electronical conductivity, unique porous structure and facile patternability. However, the majority precursor materials exhibit limited stretchability, constraining the sensitivity of the sensors [8]. A type of LIG/PDMS-based flexible strain sensors were fabricated by transferring LIG from inelastic precursors to PDMS substrates [9, 10]. The method complicates the process and results in unstable transfer effects. However, direct synthesis of LIG on PDMS by laser scribing is quite challenging on account of its low light energy absorption rate and the absence of aromatic rings [11]. The previous work synthesized LIG by laser scribing PDMS with poor conductivity [12]. The inadequate electrical conductivity of the material hinders its applications in flexible electronics and strain sensors. Alternatively, a composite film composed of lignin in a PDMS matrix was scribed by laser to synthesize conductive LIG line patterns, with lignin serving as the carbon source for graphene formation [13]. Whereas the formation of complete LIG film remains inadequate since discontinuity of lignin mixing. Consequently, in-situ synthesis of LIG with enhanced electrical conductivity on PDMS precursor is invaluable.

In this work, an enhanced electrical conductivity material, laser-induced graphene-silicon carbide laminated nanosheets (LIG-SiC LNS), is in-situ synthesized through blue-light laser scribing on MoS_2-PDMS hybrid precursor. We developed a compact flexible strain sensor utilizing LIG-SiC LNS and PDMS. The sensor with highly sensitivity and temperature stability, were used for human pulse wave monitoring and pulse wave velocity (PWV) assessment. The results exhibit practical capabilities of the sensor and broaden the potential application scenarios of the material fabrication methods.

DESIGN AND FABRICATION

Mechanism of material synthesis

The LIG-SiC LNS is synthesized by laser scribing MoS_2-PDMS hybrid precursor film. To prepare the hybrid precursors, MoS_2 powder (0.5% wt%) with particle size of ~3 μm was uniformly dispersed in uncured PDMS solution through centrifugal stirring. Curing agent was added into the mixed solution and stirred again. The mass ratio of PDMS oligomer to curing agent was 10:1. The MoS_2-PDMS hybrid precursor film was cured on a glass slide via spin-coating and heating at 80 ℃. A laser source with wavelength of 455 nm, mounted on a 3-axis electric motorized stage, was used to synthesize LIG-SiC LNS by scribing the precursor with a designed pattern. During the laser scribing process, the precursor film undergoes rapid heating and cooling due to the photothermal effect of laser. Chemical bonds of carbon and silicon atoms in PDMS were broken and recombined during this process to form the LIG-SiC LNS, meanwhile some gaseous products, such as H_2O, SO_2 and Mo_xO_{3x}, were discharged (Fig. 1a). PDMS served as the carbon and silicon source for the formation of conductive LIG-SiC. MoS_2 enhanced precursor energy absorption during laser irradiation and generated gases,

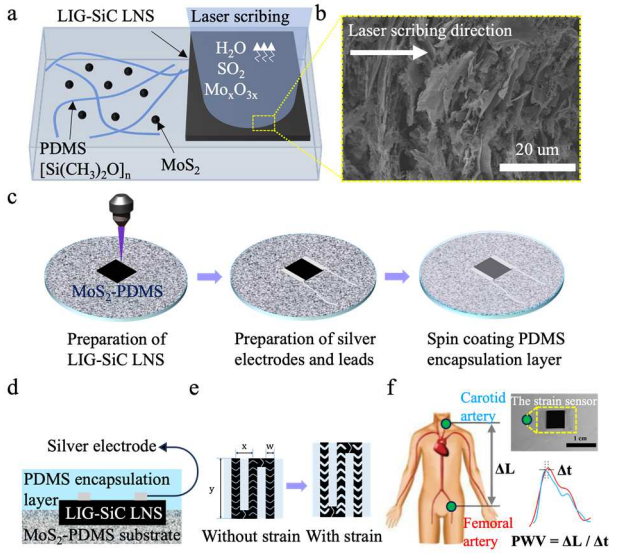

Figure 1: Schematic of material synthesis and sensor fabrication. (a) Schematic of MoS_2-PDMS precursor to LIG-SiC LNS transformation process. (b) SEM of LIG-SiC LNS. (c) Fabrication process of the strain sensor. (d) Cross-section view of the strain sensor (Side view). (e) Tensile strain sensing principle. (f) Schematic of PWV assessment using two strain sensors.

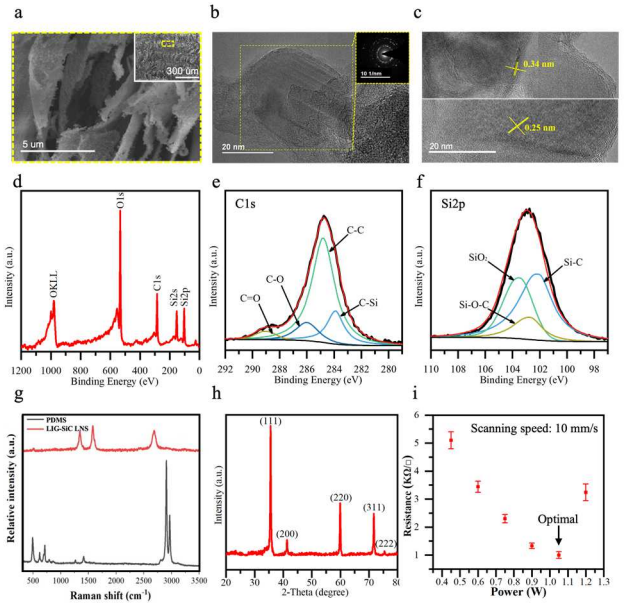

Figure 2: LIG-SiC LNS material Characterization. (a)SEM of LIG-SiC LNS. (b, c) SAED and TEM of LIG-SiC LNS. (d-f) XPS and analysis of LIG-SiC LNS. (g) Raman spectra of LIG-SiC LNS. (h) XRD pattern of LIG-SiC LNS. (i) Relationship between the sheet resistance of the composite and laser scribing power.

shaping the microstructure of the laminated nanosheets simultaneously (Fig. 1b). The direction of lamination thickness aligns with the direction of laser spot scanning.

Sensor fabrication and schematic

Based on the synthesis method of the LIG-SiC LNS mentioned above, a compact flexible strain sensor was designed and fabricated, as depicted in Fig. 1c. A square LIG-SiC LNS film measuring 6×5 mm^2 was patterned on a ~100 μm thick MoS_2-PDMS hybrid precursor film through laser direct scribing. Both ends of the square film were connected to silver wire electrodes using silver paste. A pure PDMS encapsulation layer, with a mass ratio of 10:1 for base to curing agent, was spin-coated onto the surface and cured at 80 ℃ to protect the sensitive layer. The spare PDMS was trimmed to obtain the flexible strain sensor. The cross-section schematic shows the triple-layer of the sensor (Fig. 1d). The strain sensitive LIG-SiC LNS film is sandwiched between the stretchable PDMS/ MoS_2-PDMS outer shell. The continuous LIG-SiC LNS film consists of parallel straight lines scribed by laser spot. Under applied strain, the laminated nanosheets separate and crack along the y-direction, leading to an increase in the sensor's resistance (Fig. 1e). The detailed laser and pattern-scribing parameters are recorded in Table 1. For pulse wave monitoring and PWV assessment, two sensors were affixed

Table 1: Parameters of laser source and scribing path

Laser power/W	0.45-1.2	**x/mm**	0.15
Laser scanning speed/mm·s^{-1}	7-10	**y/mm**	6
Laser spot size/mm	0.1-0.3	**w/mm**	0.135-0.15

to the skin above the carotid and femoral arteries of a volunteer respectively, as shown in Fig. 1f. The pulse wave signals of the arteries were recorded simultaneously. Thus, PWV were calculated using the following equation:

$$PWV = \Delta L / \Delta t \quad (1)$$

where ΔL is the physical distance between the monitoring points of the sensors and Δt is the time difference between the main peaks of adjacent pulse waves.

RESULT AND DISCUSSION

Material characterizations

The synthesized LIG-SiC LNS was characterized by morphology and spectral analysis. In Fig. 2a, the scanning electron microscope (SEM) image reveals that the LIG-SiC LNS consists of stacked nanosheets with a thickness of less than 100 nm. The inset highlights the ordered laminated nanosheets over a larger scale. The parallel lines scribed by the laser spot are distinctly visible. High-resolution transmission electron microscope (TEM) was employed to investigated the nano structure of the LIG-SiC LNS. The concentric rings in the selected area electron diffraction (SAED) pattern indicate the nanosheet is polycrystalline (Fig. 2b). Fig. 2c shows the lattice space of ~0.34 nm and ~0.25 nm, corresponding to the (002) planes in graphitic materials and the (111) plane of β-SiC, respectively. The X-ray photoelectron spectroscopy (XPS) spectrum shows a dominant C-C peak and C-Si (Fig. 2d-f), indicating that the LIG-SiC LNS mainly consists of sp^2-carbons and SiC. The depletion of Mo and S element peaks suggests thorough combustion of MoS_2 during the laser scribing process. Figure 2g shows representative Raman spectra of LIG-SiC LNS and pure PDMS film. The three prominent peaks of LIG-SiC LNS, D-peak at ~1,350 cm^{-1}, G-peak at ~1,580 cm^{-1} and 2D-peak at ~2,700cm^{-1}, resemble the Raman

spectra of LIG that induced from other precursors. However, the higher D-peak and wider half peak width of 2D-peak indicate more defects and poorer crystallinity of graphene in LIG-SiC compared with LIG synthesized from polyimide precursor. The X-Ray Diffraction (XRD) pattern in Figure 2h shows the β-SiC diffraction peaks. The morphology and spectra corroborate the synthesized material is composed of LIG and β-SiC. The square resistance of LIG-SiC LNS film can be modulated by adjusting laser power (Figure 2i). Increased laser power leads to enhanced material graphitization and the formation of an ordered LNS structure, leading to reduced square resistance. However, the excessive output laser power may oxidize the synthesized LIG and impair its conductivity. The minimum sheet resistance of LIG-SiC LNS is ~1 kΩ with the optimized laser parameter, showcasing a fivefold enhanced electrical conductivity compared to LIG synthesized from pure PDMS precursor.

The strain sensor performance calibrations

The sensor was stretched to a precise strain by an electric motorized stage, meanwhile the resistance was recorded by a digital multimeter. The gauge factor (GF) is calculated using the equation:

$$GF = \Delta R / R_0 \varepsilon \quad (2)$$

where ΔR is the resistance change, R_0 is the initial resistance, and ε is the applied strain. The GF of the strain sensor is 79.18 on average (Fig. 3a). Temperature typically interferes elastic strain sensors in practical applications due to signal drifts caused by substrates thermal expansion. However, owing to the negative temperature resistance coefficient of LIG-SiC LNS, the performance drifts caused by substrate thermal expansion are partially offset, providing the sensor with self-temperature compensation capability (Fig. 3b). The GF of the sensor slightly drifts within the temperature range of 20-30 ℃. The self-temperature compensation capability eliminates the need for algorithm intervention during signal processing, greatly reducing the complexity of system calibrations in actual use. The sensor exhibits a minimum detectable repetitive strain of 0.04% (Fig. 3c), showcasing the excellent strain resolution conductive to weak physiological signal detection. A response time tested from five different samples is ~40 ms on average with a minimal error bar, indicating consistent performance of the sensors (Fig. 3d). For the durability test, a sensor was stretched to a maximum strain of 5% over 10,000 cycles. The slight response attenuation indicates the reliability of the sensor for prolonged use (Fig. 3e).

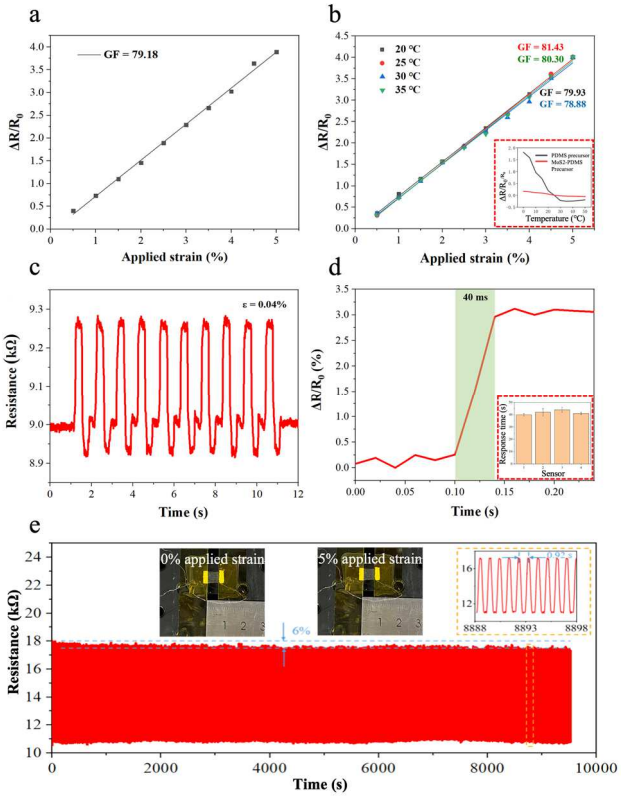

Figure 3: The performance test of the strain sensor. (a) The relatively resistance change versus applied strain. (b) Temperature effect for GF drift. (c) Minimum strain detection test. (d) Response Time for the minimum strain. (e) Repeatability and durability test.

Pulse wave and pulse wave velocity assessment

In a demonstration of physiological monitoring, the flexible strain sensors were used to detect human pulse wave signals and PWV assessment. PWV, representing the velocity of blood pressure pulse propagation through arteries, serves as an evaluation index for arterial stiffness and certain cardiovascular diseases. As shown in Fig. 4a-b, pulse wave signals from the carotid and femoral arteries of a volunteer were simultaneously recorded by two sensors. PWV results were calculated by measuring Δt between wave peaks. The average PWV for five subject numbers is 8.02 m/s (Fig. 4c). Meanwhile, a commercial PWV sensor

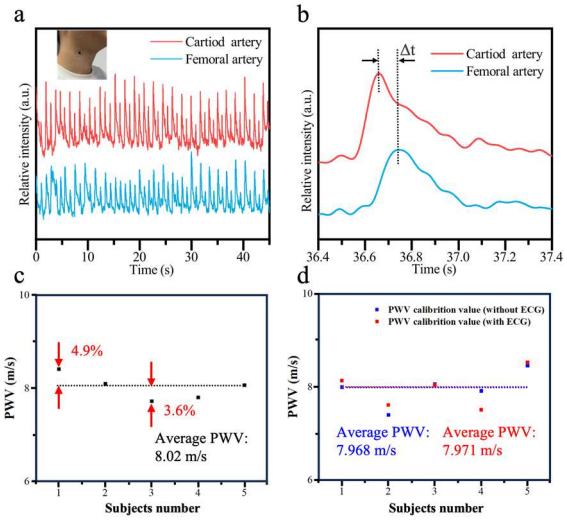

Figure 4: Physiological and PWV assessment. (a-b) Pulse waveforms of carotid and femoral artery acquired continuously using the sensor. (c) Feature point extraction results and calculated PWV values. (d) PWV calibration value measured by two different systems to evaluate detect errors.

device was used to detect PWV of the same volunteer for benchmarking (Fig. 4d). The PWV value calibrated with ECG is identified as the most accurate value. The results

demonstrate the practicality of the flexible strain sensor presented in this paper for physiological monitoring and PWV assessment, with a minimal deviation of 0.6% compared to the commercial device.

CONCLUSION

In this paper, we demonstrate a novel flexible strain sensor utilizing LIG-SiC LNS for the first time. The in-situ synthesis of LIG-SiC LNS through laser direct scribing on MoS_2-PDMS surface simplifies the sensor fabrication process. Comprehensive characterization of the LIG-SiC LNS, including morphology and composition, has been conducted. The sensor exhibits high sensitivity and intrinsic self-temperature compensation capability owing to the unique properties of LIG-SiC LNS. Experimental results demonstrate the practicality of the sensor for psychological signal detection and PWV assessments. In addition to strain sensors, this material is expected to be used in other PDMS-based electronics and microfluidic devices considering the versatility of PDMS. The electrically functional components can be easily patterned on the specific position of PDMS devices benefiting from the direct scribing and in-situ synthesis method, which will greatly enrich the functionalities of these devices.

ACKNOWLEDGEMENTS

Yixin Liu and Yanru Chen contributed equally to this work. We thank Hanxiao Liu for advices to some figures. This work is supported by the Shenzhen Fundamental Research Funds (No. JCYJ20220530143011026).

REFERENCES

[1] Z. Shen, F. Liu, S. Huang, H. Wang, C. Yang, T. Hang, J. Tao, W. Xia, and X. Xie, "Progress of flexible strain sensors for physiological signal monitoring," *Biosens. Bioelectron.,* vol. 211, pp. 114298, 2022.

[2] D. Qi, K. Zhang, G. Tian, B. Jiang, and Y. Huang, "Stretchable Electronics Based on PDMS Substrates," *Adv. Mater.,* vol. 33, pp. 2003155, 2020.

[3] J. Chen, J. Zheng, Q. Gao, J. Zhang, J. Zhang, O. Omisore, L. Wang, and H. Li, "Polydimethylsiloxane (PDMS)-Based Flexible Resistive Strain Sensors for Wearable Applications," *Appl. Sci.-Basel,* vol. 8, pp. 345, 2018.

[4] X. Wang, J. Li, H. Song, H. Huang, and J. Gou, "Highly Stretchable and Wearable Strain Sensor Based on Printable Carbon Nanotube Layers/ Polydimethylsiloxane Composites with Adjustable Sensitivity," *ACS Appl. Mater. Interfaces,* vol. 10, pp. 7371-7380, 2018.

[5] M. Amjadi, A. Pichitpajongkit, S. Lee, S. Ryu, and I. Park, "Highly Stretchable and Sensitive Strain Sensor Based on Silver Nanowire Elastomer Nanocomposite," *ACS Nano,* vol. 8, pp. 5154-5163, 2014.

[6] R. Rahimi, M. Ochoa, W. Yu, and B. Ziaie, "Highly Stretchable and Sensitive Unidirectional Strain Sensor via Laser Carbonization," *ACS Appl. Mater. Interfaces,* vol. 7, pp. 4463-4470, 2015.

[7] T. S. D. Le, H. P. Phan, S. Kwon, S. Park, Y. Jung, J. Min, B. J. Chun, H. Yoon, S. H. Ko, S. W. Kim, and Y. J. Kim, "Recent Advances in Laser-Induced Graphene: Mechanism, Fabrication, Properties, and Applications in Flexible Electronics," *Adv. Funct. Mater.,* vol. 32, pp. 2205158, 2022.

[8] S. Luo, P. T. Hoang, and T. Liu, "Direct laser writing for creating porous graphitic structures and their use for flexible and highly sensitive sensor and sensor arrays," *Carbon,* vol. 96, pp. 522-531, 2016.

[9] Y. Liu, H. Li, and M. Zhang, "Wireless Battery-Free Broad-Band Sensor for Wearable Multiple Physiological Measurement," *ACS Appl. Electron. Mater.,* vol. 3, pp. 1681-1690, 2021.

[10] Y. Wu, I. Karakurt, L. Beker, Y. Kubota, R. Xu, K. Y. Ho, S. Zhao, J. Zhong, M. Zhang, X. Wang, and L. Lin, "Piezoresistive stretchable strain sensors with human machine interface demonstrations," *Sens. Actuator A-Phys.,* vol. 279, pp. 46-52, 2018.

[11] S. Hayashi, F. Morosawa, and M. Terakawa, "Synthesis of silicon carbide nanocrystals and multilayer graphitic carbon by femtosecond laser irradiation of polydimethylsiloxane," *Nanoscale Adv.,* vol. 2, pp. 1886-1893, 2020.

[12] Y. Zhu, H. Cai, H. Ding, N. Pan, and X. Wang, "Fabrication of Low-Cost and Highly Sensitive Graphene-Based Pressure Sensors by Direct Laser Scribing Polydimethylsiloxane," *ACS Appl. Mater. Interfaces,* vol. 11, pp. 6195-6200, 2019.

[13] K. Sinha, L. Meng, Q. Xu, and X. Wang, "Laser induction of graphene onto lignin-upgraded flexible polymer matrix," *Mater. Lett.,* vol. 286, pp. 129268, 2021.

CONTACT

*Min Zhang, tel: +86-18038153135;
zhang.min@sz.tsinghua.edu.cn